JOURNAL OF GUIDANCE, CONTROL, AND DYNAMICS
Vol. 21, No. 4, July–August 1998

Engineering Notes

ENGINEERING NOTES are short manuscripts describing new developments or important results of a preliminary nature. These Notes cannot exceed 6 manuscript pages and 3 figures; a page of text may be substituted for a figure and vice versa. After informal review by the editors, they may be published within a few months of the date of receipt. Style requirements are the same as for regular contributions (see inside back cover).

Virtual Flight Data Recorder: A Neural Extension of Existing Capabilities

Marcello R. Napolitano,* Dale A. Windon,†
David R. Martinelli,‡ and José L. Casanova§
West Virginia University,
Morgantown, West Virginia 26506-6106

Introduction

FEDERAL Aviation Administration (FAA) rules in effect up to July 1997 mandated the aircraft flight data recorder (FDR) to record a certain number of dynamic time histories. These usually include airspeed, altitude, Euler angles, and linear accelerations. However, the recorded parameters do not include the deflections of the control surfaces. The absence of these data can potentially be critical in the event of a crash investigation. This Note proposes the introduction of a neural network- (NN-) based scheme to reconstruct these important time histories. Particularly, the scheme consists of an NN simulator (NNS) and an NN reconstructor (NNR). The NNS is trained, using available flight data for the particular aircraft, to simulate any desired dynamic output recorded in current FDRs and then interfaced with an NNR. The outputs of the NNR are the control surface deflections (or any other parameter of interest not recorded by the FDR), which minimize a performance index based on the differences between the available data from the FDR and the output from the NNS. The scheme has been tested with flight data from a Boeing 737-300. The combination of the NNS and the NNR leads to the concept of a virtual flight data recorder (VFDR). The VFDR approach assumes the availability of a single aircraft equipped with an FDR with extended recording capabilities for each aircraft operated by the airlines. The VFDR can be evaluated as a tool for crash investigations, where loss of control is believed to be a factor.

Neural Network Simulator

An NN can be defined as an approximated mathematical model of the human brain's problem solving activities.[1] In recent years there have been numerous studies focusing on applications of NNs to a variety of flight control problems. Particularly, NNs have been proposed for fault-tolerant flight control systems (following actuator and sensor failure), autopilot and stability augmentation systems, and aircraft parameter estimation from flight data. In this Note a feedforward NN with supervised learning is used. For the purpose of this study, two of the key NN properties of interest are their applicability to nonlinear systems,[2] due to their mapping capabilities, and their applicability to multivariable systems because NNs are, by definition, multi-input/multi-output entities. The off-line learning implemented to achieve the mapping between input and output data within the VFDR is performed through the application of the extended back-propagation algorithm.[3] A complete set of dynamic data from a Boeing 737-300 equipped with an extended FDR was kindly provided by the National Transportation Safety Board (NTSB) following a request by the first author. The 14,000-s dynamic time histories included the following parameters: ϕ, θ, Ψ, a_n, a_x, a_y, calibrater air speed (CAS), altitude, N_1, δ_E, δ_A, δ_R, δ_{TEF}, δ_{LEF}, and δ_{LES}, where N_1 is the percentage of the engines maximum revolutions per minute. Typical FDRs only record a subset of these parameters. For the purpose of the study, it was assumed that the following parameters are recorded by a typical FDR: ϕ, θ, ϕ, a_n, a_x, a_y, CAS, and altitude.

The Boeing 737-300 features on each wing two trailing-edge (TE) flaps, two leading-edge (LE) flaps, and two LE slats. The deflections of the LE surfaces are scheduled with the deflection of the TE flaps, and the TE flaps are scheduled as a function of the airspeed. The aircraft also features flight spoilers and ground spoilers, which were not activated during these flight tests. The sampling frequencies varied greatly among the different parameters from 1 to 8 samples/s. Therefore, prior to the NN training, the data underwent a cubic interpolation to have the same sampling frequency of 8 samples/s for each time history. A fifth-order digital Butterworth filter was then applied to the interpolated data to reduce the noise level. The cutoff frequencies were carefully selected to avoid removing significant portions of the aircraft rigid-body dynamics. Reference 4 provided general guidelines for selecting the NNS architecture. Therefore, architectures with a single hidden layer, with a number of hidden neurons slightly higher than the number of input data, and with low learning rates were considered. Excluding the takeoff, climbing, descent, and landing phases, there were approximately 10,500 s of maneuvered flight. The training for the NNS was conducted using 7500 s of data with the remaining 3000 s being used for the testing of the NNS. The training consisted of submitting the 7500-s training data to the NNS for a total of 250 iterations. The training, performed with decreasing learning rates, was monitored by freezing the numerical architecture of the NNS every 10 iterations and by letting the frozen NNS go through the first 1000 s of testing data. The following classical statistical parameters for the estimation error associated with the simulation were introduced:

$$\mu_{\text{simul}} = \frac{\sum_{i=1}^{N}(X_{\text{simul}} - X_{\text{FDR}})}{N}$$
$$\sigma^2_{\text{simul}} = \frac{\sum_{i=1}^{N}[(X_{\text{simul}} - X_{\text{FDR}}) - \mu_{\text{simul}}]}{N} \tag{1}$$

where X indicates any of the NNS outputs and N is the total number of data points for the testing phase ($N = 1000 \times 8$ samples/s $= 8000$). Figure 1 shows the statistical trend of the NNS estimation error variance for the 250 iterations revealing a desirable decreasing trend; however, the presence of a persistent asymptotic variance for the roll angle estimation error was of some concern because it can lead to substantial error in the reconstruction of the rolling dynamics. A careful analysis of the FDR ailerons data revealed some difference between the magnitudes of the left and right aileron recordings. Furthermore, this difference was not consistent throughout the flight, ranging between 1 and 4 deg; therefore, it could not be treated as a

Received Nov. 5, 1996; revision received Feb. 4, 1998; accepted for publication Feb. 18, 1998.

*Associate Professor and Aviation Operation and Safety Center Director, Department of Mechanical and Aerospace Engineering. Member AIAA.

†Graduate Research Assistant, Aviation Operation and Safety Center, Department of Mechanical and Aerospace Engineering. Student Member AIAA.

‡Associate Professor and Harley Staggers National Transportation Director, Department of Civil and Environmental Engineering.

§Graduate Research Assistant, Aviation Operation and Safety Center, Department of Mechanical and Aerospace Engineering. Member AIAA.

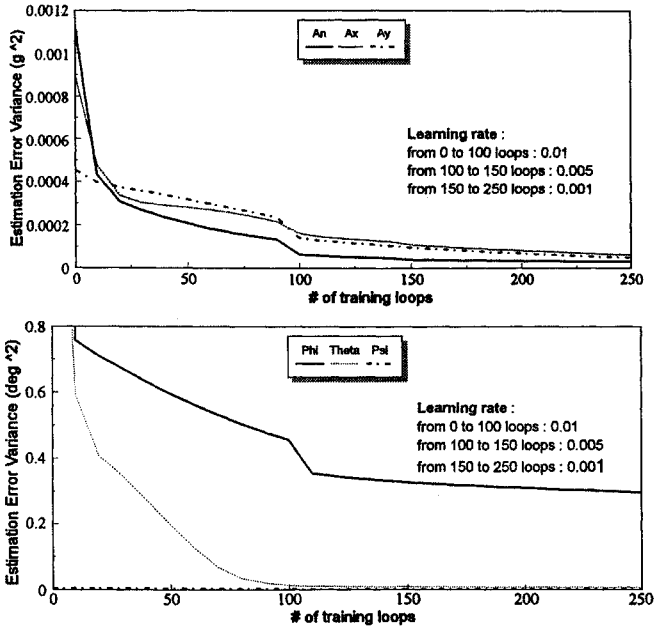

Fig. 1 Variance of the NNS simulation error vs number of training loops for the linear accelerations and the Euler angles.

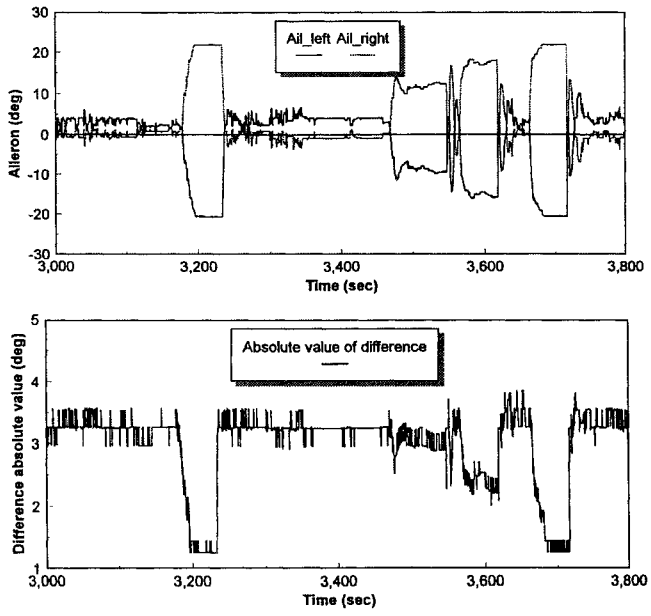

Fig. 2 Analysis of the raw FDR ailerons data.

removable bias. Figure 2 shows a comparison of the raw left and right aileron deflections along with the magnitude of their difference for generic 500 s of the training data. Most likely this difference was due to a minor calibration problem for the right and left aileron channels of the data acquisition system. The raw data for the deflections of left and right elevators and spoilers were also checked for a similar problem showing no significant inconsistency. Although the occurrence of this type of problems may not be uncommon, it is significant that the NNS was able to detect this anomaly in the rolling dynamics, as shown in Fig. 1.

Neural Network Reconstructor

For reconstructing the deflections of the control surfaces, a multi-input/multi-output NNR was introduced. The inputs to the NNR are given by the NNS output data or by a subset of these data. The NNR outputs are the estimates of the deflections of the control surfaces at time instant k, which minimize the differences between the NNS time histories and those from the FDR at time instant $k+1$. The process is iterative, and the reconstruction scheme proceeds to the next time step only when the deflections of the control surfaces at

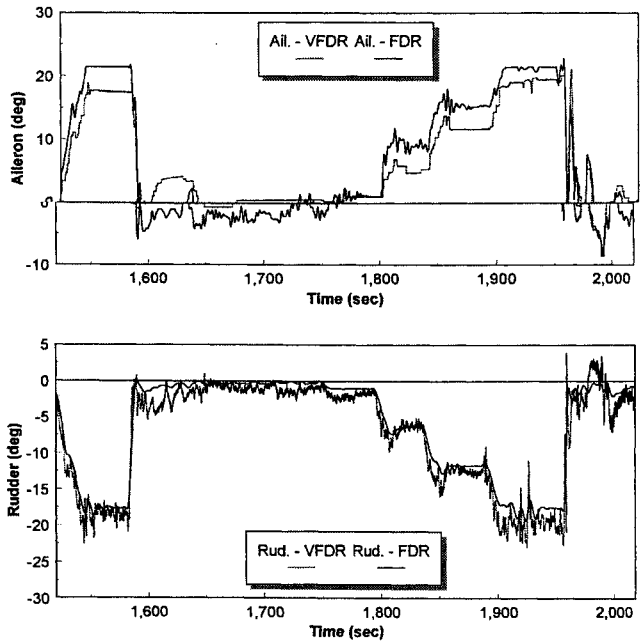

Fig. 3 Comparison between NNR and FDR time histories for ailerons and rudder deflections.

time k, minimizing the FDR and NNS time histories at time $k+1$, are found by the NNR. For the study the attention was focused on the reconstruction of the lateral-directional control surfaces. Several configurations for the cost functions to be minimized at the output layer were considered. The results presented are relative to the following cost functions:

$$J_{\text{lat}}(k) = a_1[\phi_{\text{FDR}}(k+1) - \phi_{\text{NNS}}(k+1)] \tag{2}$$

$$J_{\text{dir}}(k) = b_1[\Delta\psi_{\text{FDR}}(k+1) - \Delta\psi_{\text{NNS}}(k+1)] \tag{3}$$

where $a_1 = -10$, $b_1 = 10$, and $\Delta\psi(k+1) = \psi(k+1) - \psi(k)$. The following statistical parameters for the reconstruction error were introduced:

$$\mu_{\text{recon}} = \frac{\sum_{i=1}^{N}\left(\delta_{x_{\text{NNR}}} - \delta_{x_{\text{FDR}}}\right)}{N}$$

$$\sigma^2_{\text{recon}} = \frac{\sum_{i=1}^{N}\left[\left(\delta_{x_{\text{NNR}}} - \delta_{x_{\text{FDR}}}\right) - \mu_{\text{recon}}\right]^2}{N} \tag{4}$$

where $x = A$ (ailerons) or R (rudder) and N is, again, the total number of discrete data points. Of course, in an application of the method to actual flight data, the FDR control surface deflections are not available and are the objectives of the reconstruction. Figure 3 shows the reconstruction for the aileron and rudder deflection time histories during 500 s of the testing data. It can be seen that the reconstructed deflections are able to follow the actual deflections of the control surfaces within some approximation. The error in the reconstruction of the aileron deflections should not be surprising due to the presence of a nonnegligible difference between the left and right aileron readings as already described.

Conclusions

This Note has presented an approach for the reconstruction of control surface deflections inasmuch as these parameters, according to FAA rules in effect up to July 1997, were not recorded by FDRs for aircraft built prior to 1989. The methodology takes advantage of the capabilities offered by NNs for nonlinear mapping purposes. Specifically, the approach is based on the development of an NNR that provides estimates of the control surface deflections minimizing weighted quadratic differences, at each computational time step, between the actual time histories from an FDR and the simulated time histories from a parallel nonlinear simulation, also NN based. The approach was tested with actual Boeing 737-300 flight data provided by the NTSB.

Acknowledgment

The authors wish to thank the National Transportation Safety Board (NTSB) for the B737-300 data provided for this study.

References

[1]Rumelhart, D., and McClelland, J., *Parallel Distributed Processing*, MIT Press, Cambridge, MA, 1986, pp. 318–330.

[2]Narendra, K. S., and Partasarathy, K., "Identification and Control of Dynamical Systems Using Neural Networks," *IEEE Transactions on Neural Networks*, Vol. 1, No. 1, 1990, pp. 4–27.

[3]Chen, C. L., and Nutter, R. S., "An Extended Back-Propagation Learning Algorithm by Using Heterogeneous Processing Units," *Proceedings of the International Joint Conference on Neural Network*, IJCNN '92 (Baltimore, MD), Vol. 3, Inst. of Electrical and Electronics Engineers, 1992, pp. 988–993.

[4]De Villiers, J., and Barnard, E., "Back-Propagation Neural Nets with One and Two Hidden Layers," *IEEE Transactions on Neural Networks*, Vol. 4, Feb. 1993, pp. 136–141.

Frequency Weighting for the H_∞ and H_2 Control Design of Flexible Structures

W. Gawronski*
Jet Propulsion Laboratory, California Institute of Technology, Pasadena, California 91109
and
K. B. Lim†
NASA Langley Research Center, Hampton, Virginia 23665

Introduction

THE H_∞ and the related H_2 controller design methodologies allow for the design of control systems that meet tracking requirements and, at the same time, maintain the binding disturbance rejection properties. To achieve this, the problem should be appropriately defined in the quantitative terms. For example, the frequency shaping filters are used to define tracking requirements or disturbance rejection performance of the closed-loop system. These frequency-dependent weights filters are used only in the controller design stage. They add to the complexity of the problem because in the process of design the number of system equations varies and their parameters are modified. As stated by Voth et al. in Ref. 1, p. 55, "The selection of the controller gains and filters as well as the controller architecture is an iterative, and often tedious, process which relies heavily on the designers' experience." It is shown in this Note that this task is simplified in the case of flexible structure control. If a structure model is in the modal representation, then the addition of a filter is equivalent to the multiplication of each row of the plant input matrix by a constant. The ith constant is the filter gain at the ith natural frequency of the structure. In this way, each natural mode is weighted separately. This approach addresses the system performance at the mode level, which simplifies what otherwise may be an ad hoc and tedious process.

Properties of Flexible Structures and Filters

We assume that a flexible structure is in the modal representation. Its transfer function G has the state space representation (A, B, C), with n degrees of freedom (or number of flexible structure modes), $2n$ states, p inputs, and q outputs. Denote ω_i the ith natural frequency and ζ_i the ith modal damping, $i = 1, \ldots, n$. We assume low damping ($\zeta_i < 0.1$ for all modes) and distinct natural frequencies. In the modal representation, the system matrix A is block diagonal with 2×2 blocks on the diagonal, and B and C are divided into $2 \times p$ and $q \times 2$ blocks (see Ref. 2, pp. 12–14):

$$A = \operatorname{diag}(A_i), \qquad B = \begin{bmatrix} B_1 \\ B_2 \\ \vdots \\ B_n \end{bmatrix}, \qquad C = [C_1 \quad C_2 \quad \cdots \quad C_n] \tag{1}$$

$$A_i = \begin{bmatrix} -\zeta_i\omega_i & \omega_i \\ -\omega_i & -\zeta_i\omega_i \end{bmatrix}$$

where $i = 1, \ldots, n$. Denote the transfer function of the ith mode as $G_i = C_i(j\omega I - A_i)^{-1}B_i$, then one obtains the following decomposition of transfer function in modal coordinates:

$$G(\omega) = \sum_{i=1}^{n} G_i(\omega) \tag{2a}$$

$$G(\omega_i) \cong G_i(\omega_i), \qquad i = 1, \ldots, n \tag{2b}$$

Equation (2a) can be derived by introducing A, B, and C as in Eq. (1) to the definition of the transfer function. Equation (2b) follows from Eq. (2a), by noting that the response at frequency ω_i is dominated by the ith mode, that is, $\|G_j(\omega_i)\|_2 \ll \| G_i(\omega_i)\|_2$ for $i \neq j$.

Consider a filter, with a diagonal transfer function $F(\omega)$. The diagonal input (output) filter represents lack of coupling between the inputs (or outputs). Denote α_i the magnitude of the filter response at the ith natural frequency, $\alpha_i = |F(\omega_i)|$. The filter is smooth if the slope of its transfer function near the structural resonance is small when compared to the slope of the structure near the resonance. With these assumptions, the following property of the H_∞ norm of a structure with a filter is valid:

$$\|G\|_\infty \cong \max_{i \in [1,n]} (\|G_i\|_\infty) \tag{3a}$$

$$\|GF\|_\infty \cong \max_{i \in [1,n]} (\|G_i\alpha_i\|_\infty) \tag{3b}$$

To prove Eq. (3a), note that

$$\|G\|_\infty = \sup_\omega \bar{\sigma}(G(\omega)) \cong \max_{i \in [1,n]} \bar{\sigma}(G(\omega_i)) \cong \max_{i \in [1,n]} \bar{\sigma}(G_i(\omega_i)) \tag{4a}$$

Both approximations in Eq. (4a) hold because the resonance response of the ith mode dominates the structural response, as given in Eq. (2). However, because $\|G_i\|_\infty \cong \bar{\sigma}(G_i(\omega_i))$, therefore, Eq. (3a) is valid. To prove Eq. (3b), note that for the smooth F the transfer function GF preserves the properties of a flexible structure given by Eq. (2); thus,

$$\|GF\|_\infty = \sup_\omega \bar{\sigma}[G(\omega)F(\omega)] \cong \max_{i \in [1,n]} \bar{\sigma}[G(\omega_i)F(\omega_i)]$$
$$\cong \max_{i \in [1,n]} \bar{\sigma}(G_i(\omega_i)\alpha_i) \tag{4b}$$

In the preceding approximation we took into consideration that $\sigma_k(GF) = \sigma_k(G|F|)$, which can be proven as follows:

$$\sigma_k^2(GF) = \lambda_k(F^*G^*GF) = \lambda_k(FF^*G^*G) = \lambda_k(|F|^2G^*G)$$
$$= \lambda_k(|F|G^*G|F|) = \sigma_k^2(G|F|) \tag{4c}$$

Equation (3) says that the largest modal peak response of a lightly damped structure determines the worst-case response. A similar property holds for the 2-norm of a structure with a filter

$$\|G\|_2^2 \cong \sum_{i=1}^{n} \|G_i\|_2^2 \tag{5a}$$

$$\|GF\|_2^2 \cong \sum_{i=1}^{n} \|G_i\alpha_i\|_2^2 \tag{5b}$$

Received Aug. 6, 1997; revision received Jan. 12, 1998; accepted for publication Feb. 17, 1998.

*Senior Member of the Technical Staff, Communications Ground Systems Section, M.S. 238-528. E-mail: wodek.k.gawronski@jpl.nasa.gov. Member AIAA.

†Research Engineer, Guidance and Control Branch. E-mail: k.b.lim@larc.nasa.gov. Member AIAA.